

The VLT-FLAMES Tarantula Survey

Jorick S. Vink¹, C.J. Evans², J. Bestenlehner^{1,3}, C. McEvoy⁴, O. Ramírez-Agudelo², H. Sana⁵, F. Schneider⁶ and VFTS

¹Armagh Observatory, College Hill, BT61 9DG, Armagh, Northern Ireland
email: jsv@arm.ac.uk ²ATC, Royal Observatory Edinburgh, Blackford Hill, Edinburgh, EH9 3HJ, UK ³Department of Physics and Astronomy University of Sheffield, Sheffield, S3 7RH, UK ⁴ARC, School of Mathematics and Physics, QUB, Belfast BT7 1NN, UK ⁵Institute of Astrophysics, KU Leuven, Celestijnenlaan 200D, 3001, Leuven, Belgium ⁶Department of Physics, University of Oxford, Keble Road, Oxford OX1 3RH, UK

Abstract. We present a number of notable results from the VLT-FLAMES Tarantula Survey (VFTS), an ESO Large Program during which we obtained multi-epoch medium-resolution optical spectroscopy of a very large sample of over 800 massive stars in the 30 Doradus region of the Large Magellanic Cloud (LMC). This unprecedented data-set has enabled us to address some key questions regarding atmospheres and winds, as well as the evolution of (very) massive stars. Here we focus on O-type runaways, the width of the main sequence, and the mass-loss rates for (very) massive stars. We also provide indications for the presence of a *top-heavy* initial mass function (IMF) in 30 Dor.

Keywords. stars: early-type, stars: massive, stars: evolution, stars: luminosity function, mass function, stars: mass loss, stars: fundamental parameters

1. Introduction

Massive star evolution is important for many fields of Astrophysics including supernovae (SNe; Levesque, these proceedings). Yet, it remains largely unconstrained (Langer 2012; Meynet these proceedings). Progress can be made using high-quality observations from nearby sources, as well as from large data-sets such as VFTS (Evans et al. 2011) discussed here. In parallel, VFTS data are analysed using state-of-the-art model atmospheres such as CMFGEN (Hiller & Miller 1998) and FASTWIND (Puls et al. 2005), as well as automatic fitting tools (Sabín-Sanjulián et al. 2014; Bestenlehner et al. 2014; Ramírez-Agudelo et al. 2017).

In addition to this observational progress, our VFTS collaboration strives to make theoretical progress on stellar winds and evolution, and we are in the unique position to confront our new models against VFTS data. In the following, we highlight a number of recent results that we argue make a real difference to our knowledge of massive stars.

1.1. Motivation for the Tarantula region

The Tarantula region (30 Doradus) is the largest active star-forming region in our Local Universe for which individual spectra of the massive-star population can be obtained. Because it is the largest region, it provides a unique opportunity to study the most massive stars, including very massive stars (VMS) with masses up to 200-300 M_{\odot} (Crowther et al. 2010; Bestenlehner et al. 2014; Martins 2015; Vink et al. 2015). This allows us to properly investigate whether the upper-IMF may be top-heavy (Schneider et al. 2017). Answering this question is important as these VMS that are thought to dominate the ionizing radiation and wind feedback from massive stars (Doran et al. 2013).

Another reason to study 30 Doradus is that testing massive star evolution *requires*

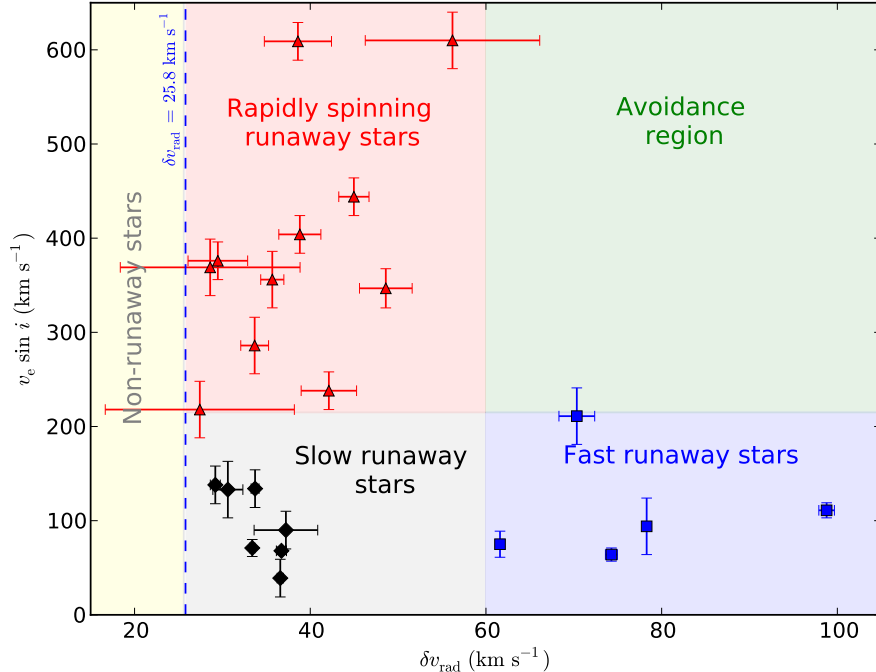


Figure 1. Rotational velocities of both slow & fast runaways (Sana et al. in prep.). Whilst there are slow runaways at high $v \sin i$, and fast runaways at relatively low $v \sin i$, there appears to be a Region-of-Avoidance for fast runaways with large $v \sin i$. These diagnostics might enable us to disentangle the different proposed origins for runaways, as discussed in the text.

large data-sets. For instance, the issue of the location of the terminal-age main sequence (TAMS) can only be addressed when the sample-size is sufficiently large to populate both the main-sequence with O-type stars (Sabín-Sanjulián et al. 2017; Ramírez-Agudelo et al. 2017) and B supergiants (McEvoy et al. 2015).

2. Results on binarity, rotation rates, and runaways

The aims of VFTS were to determine the stellar parameters, such as T_{eff} , $\log g$ & $\log L$ to place our objects on the HR-diagram; the mass and \dot{M} to determine the evolution & fate of massive stars; and the helium (He) and nitrogen (N) abundances to test (rotational) mixing processes (Grin et al. 2016; Rivero-Gonzalez et al. 2012). All these parameters require sophisticated atmosphere modeling, but VFTS also offered some model-independent parameters including the rotational velocities $v \sin i$ and radial velocities (RVs) thanks to the multi-epoch nature of the survey. The latter allowed us to obtain information on the $\sim 50\%$ frequency in 30 Dor (Sana et al. 2013) and the opportunity to study the dominant mechanism for runaways (Fig. 1; Sana et al. in prep.).

Figure 1 might allow us to disentangle the dynamical runaway scenario (Gies & Bolton 1986) from the binary-SN kick scenario (Stone 1991), as the first scenario might produce relatively fast runaways, whilst one would expect the binary SN kick scenario to produce rapid rotators. Obviously, definitive conclusions can only be obtained when more sophisticated models become available.

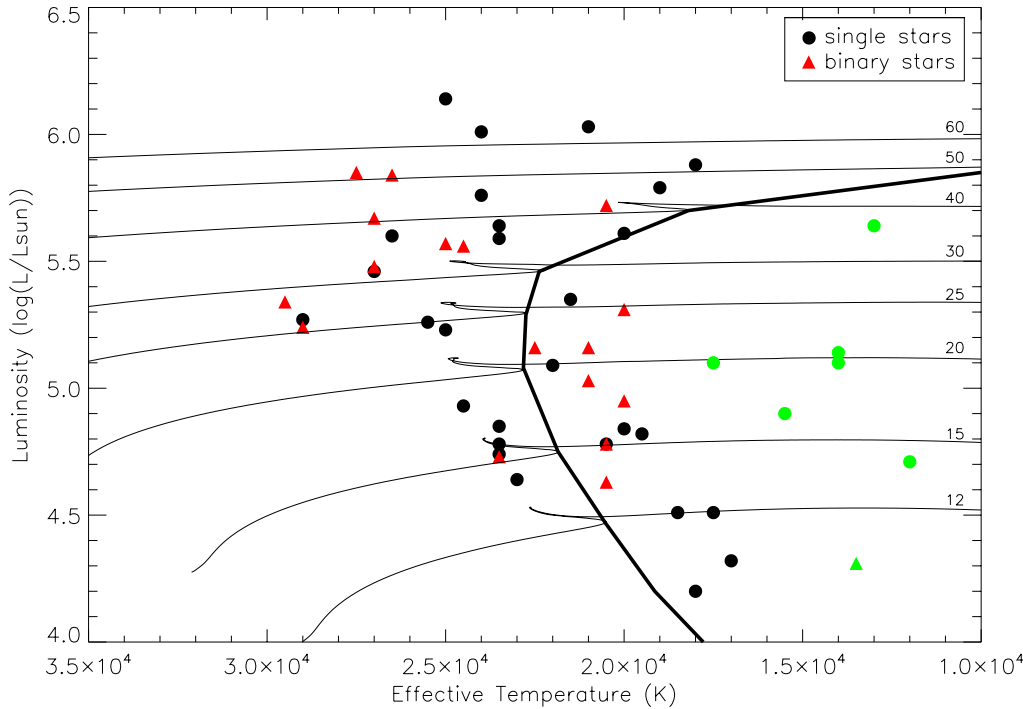


Figure 2. A zoomed-in version of the Hertzsprung-Russell diagram for single (circle) and binary (triangle) B supergiants from McEvoy et al. (2015). Also shown are the LMC evolutionary tracks of Brott et al. (2011) for $v_{\text{rot}} \simeq 225$ km/s, with the initial mass (in units of the solar mass) given on the right hand side. The dark line represents the TAMS (terminal age main sequence). The stars highlighted in green are far enough from the TAMS line that they may be interpreted as core He-burning objects.

3. The width of the main-sequence and constraints on core overshooting

Figure 2 shows a zoomed-in version of the Hertzsprung-Russell diagram for both single and binary B supergiants from McEvoy et al. (2015). The position of the dark line indicates the position of the TAMS, with its location is determined by the value of the core overshooting parameter (α_{ov}) which is basically a “free” parameter (e.g. Vink et al. 2010; Brott et al. 2011) until astro-seismology on a large number of OB supergiants becomes available. The Brott et al. models employ a value of $\alpha_{\text{ov}} = 0.335$, whilst the Geneva models (Georgy these proceedings) employ a smaller value. The VFTS results shown in Fig. 2 appear to suggest a *larger* value of α_{ov} than 0.335.

Larger α_{ov} makes bi-stability braking (BSB; Vink et al. 2010; Keszthelyi et al. 2017) feasible, which we test by showing $v \sin i$ of both VFTS and previous FLAMES-I results (Hunter et al. 2008) versus T_{eff} in Fig. 3. Note the presence of another “Region-of-Avoidance” †, where rapidly-rotating “cool” (cooler than the bi-stability location of 20 000 K; Petrov et al. 2016) B supergiants are simply not observed. The reason for this avoidance below 20 000 K could either involve BSB, or it might be that the slowly rotating cool B supergiants are He-burning objects (due to post red-supergiant evolution or binarity).

† The perceived lack of rapid rotators on the hot side of the diagram is not real, there are many rapidly rotating O-type stars. These O-stars are just not included here.

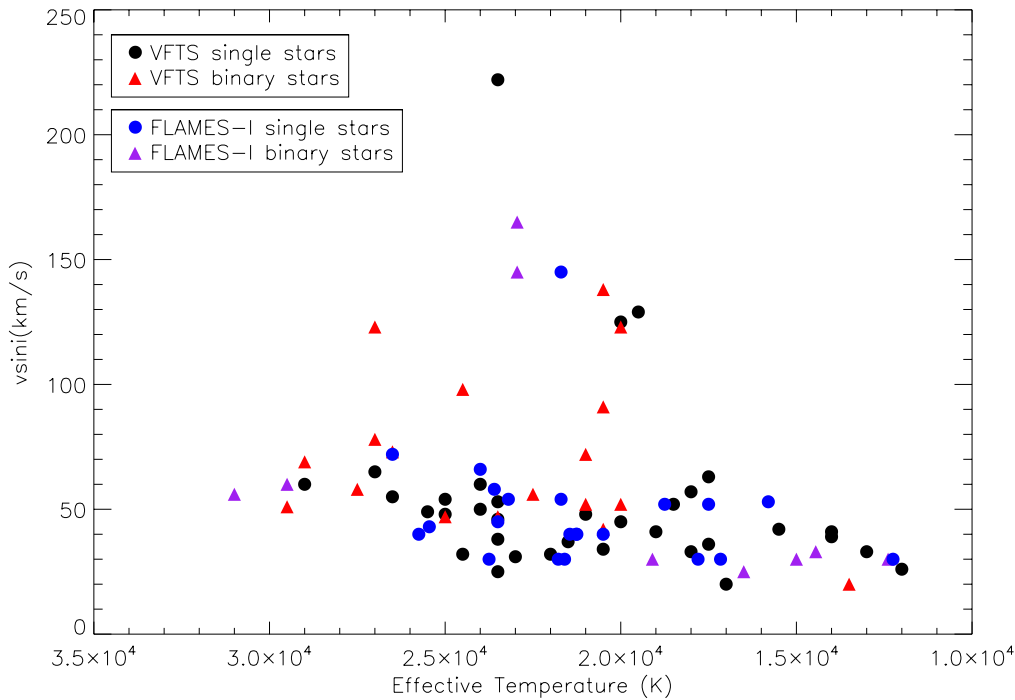


Figure 3. Effective temperatures plotted against $v \sin i$ for FLAMES-I and VFTS B-type supergiants in the LMC (see Vink et al. 2010; McEvoy et al. 2015). The perceived lack of rapid rotators on the hot side of the diagram is not real, there are many rapidly rotating O-type stars; they are just not included here.

4. The mass-loss rates

The mass-loss rates for O-type dwarfs were discussed by Sabín-Sanjulián et al. (2014; 2017), whilst those for the O giants and supergiants are plotted in the form of the wind-momentum-luminosity relation (WLR; Kudritzki & Puls 2000; Puls et al. 2008) in Fig. 4. Interestingly, the empirical WLR lies above the theoretical WLR (of Vink et al. 2001). Usually a discrepancy between theoretical and empirical values would be interpreted such that the theoretical rates would be too low, but here it is different, as it is widely accepted that empirical modeling is more dependent on wind clumping and porosity than theory (see Muijres et al. 2011 for theoretical expectations).

Indeed, it is more likely that the empirical WLR is too high, as a result of wind clumping, which has not been included in the analysis. This would imply that the empirical WLR would need to be lowered by a factor \sqrt{D} , where D is the clumping factor, which is as yet uncertain. However, given the model-independent (from clumping & porosity) transition mass-loss rate (Vink & Gräfener 2012; next Sect.) a value of $D \simeq 10$ (with a mass-loss rate and WLR reduction of ~ 3) would bring the empirical WLR and theory in reasonable agreement. None of this means that the theoretical rates for lower mass-and-luminosity O stars need necessarily to be correct. Therefore, spectral analysis of large data-sets of O-stars including clumping & porosity (Surlan et al. 2013; Sundqvist et al. 2014) are needed to provide definitive answers.

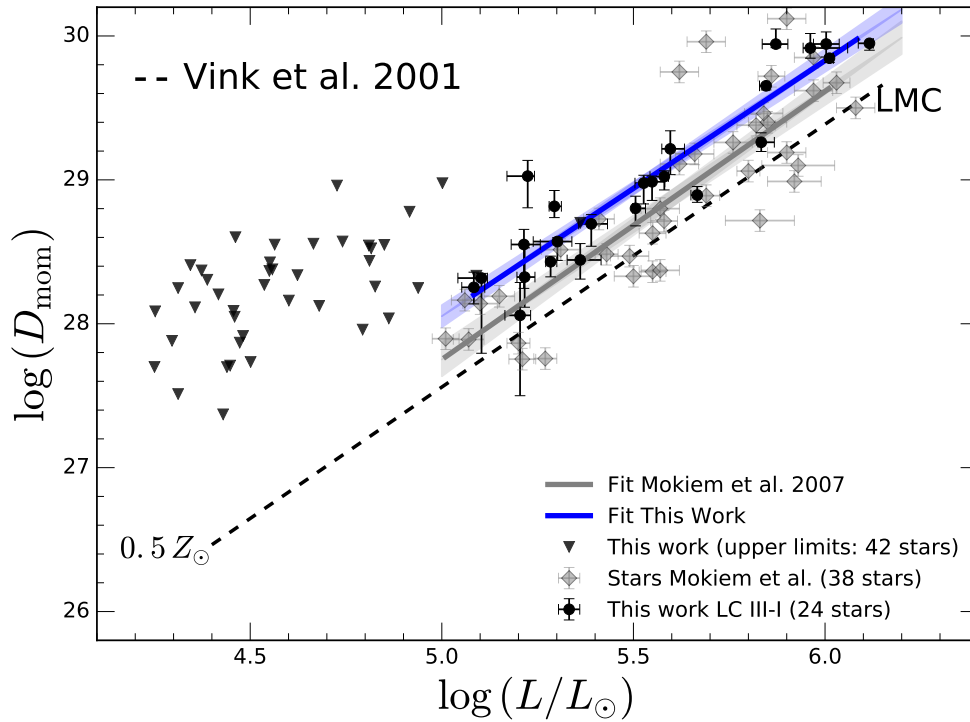


Figure 4. Modified wind momentum (D_{mom}) versus luminosity diagram from Ramírez-Agudelo et al. (2017). The dashed lines indicate the theoretical predictions of Vink et al. (2001) for homogeneous winds. The empirical fit and Mokiem et al. (2007) (both for $L/L_{\odot} > 5.0$) are shown in shaded blue and gray bars, respectively. For stars with $L/L_{\odot} \leq 5.0$, only upper limits could be constrained.

5. Very Massive Stars

The most massive stars in VFTS were analysed by Bestenlehner et al. (2014), plotted in the HRD of Fig. 5. Over-plotted are VMS evolutionary tracks and the location of the ZAMS. The HRD shows the presence of 12 VMS (with $M > 100 M_{\odot}$; Vink et al. 2015), which enables us to derive the upper-IMF of 30 Dor for the first time. Figure 6 compares the preferred value for the mass function to that of Salpeter. It is found that the slope is different to that of Salpeter (at $\sim 85\%$ confidence), and also that a Salpeter IMF cannot reproduce the larger number of massive stars above $30 M_{\odot}$ at $>99\%$ confidence (Schneider et al. 2017). As this result is obtained using the largest spectroscopic dataset ever obtained, and analysed with the most sophisticated analysis tools, we consider this the most robust test to date. A top-heavy IMF would have major implications for the interpretation of spectral modelling of high-redshift galaxies, as well as the ionizing radiation and kinetic wind energy input into galaxies. Answers will strongly depend on the mass-loss rates of these VMS, as discussed next.

Figure 7 shows VFTS results of the mass-loss rates of the most massive stars in 30 Dor (Bestenlehner et al. 2014). Whilst at relatively low values of the Eddington value Γ , the slope of the empirical data is consistent with that for O stars, those above the crossover point are not. Here the mass-loss rate kinks upwards, with a steeper slope. The winds have become optically thick, and show WR-like spectra. Also, above this critical Γ point, the wind efficiency crosses unity, enabling a calibration of the absolute mass-loss rates

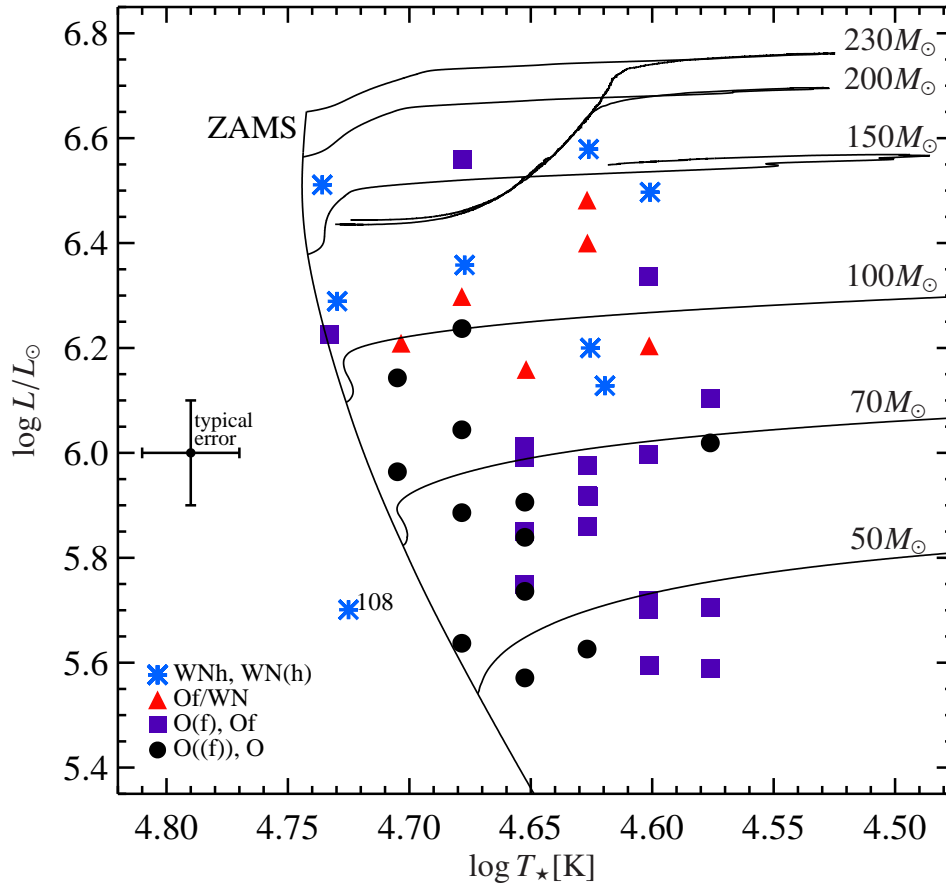


Figure 5. Distribution of spectral types of the sample of Bestenlehner et al. (2014) in the HR-diagram. The different symbols indicate different stellar sub-classes. Black lines indicate evolutionary tracks from Köhler et al. (2015) for an initial rotation rate of 300 km s^{-1} and the location of the Zero-Age Main Sequence (ZAMS).

for the first time (Vink & Gräfener 2012). Moreover, Bestenlehner et al. (2014) found profound changes in the surface He abundances exactly coinciding with the luminosity threshold where mass loss is enhanced. This suggests that Of/WN and WNh stars are objects whose H-rich layers have been stripped by enhanced mass-loss during their main-sequence life. Note that this mass-loss enhancement for VMS has not been included in most stellar evolution calculations, and this implies there will be many exciting surprises for extra-galactic applications of massive stars in the near future!

6. Final Words

The VFTS has conclusively shown that binaries are common in 30 Dor. With a corrected close-binary fraction of $\sim 50\%$ (Sana et al. 2013), we do not yet know whether this hints at a lower binary frequency at low metallicity, or it is still consistent with the larger Galactic frequency of $\sim 70\%$ when evolutionary considerations are taken into account. Either way, we now know we require both single & binary evolutionary models to make progress. Another interesting finding is that there is a high-velocity tail present in single O-type supergiants (Ramírez-Agudelo et al. 2013), which is not present in the spec-

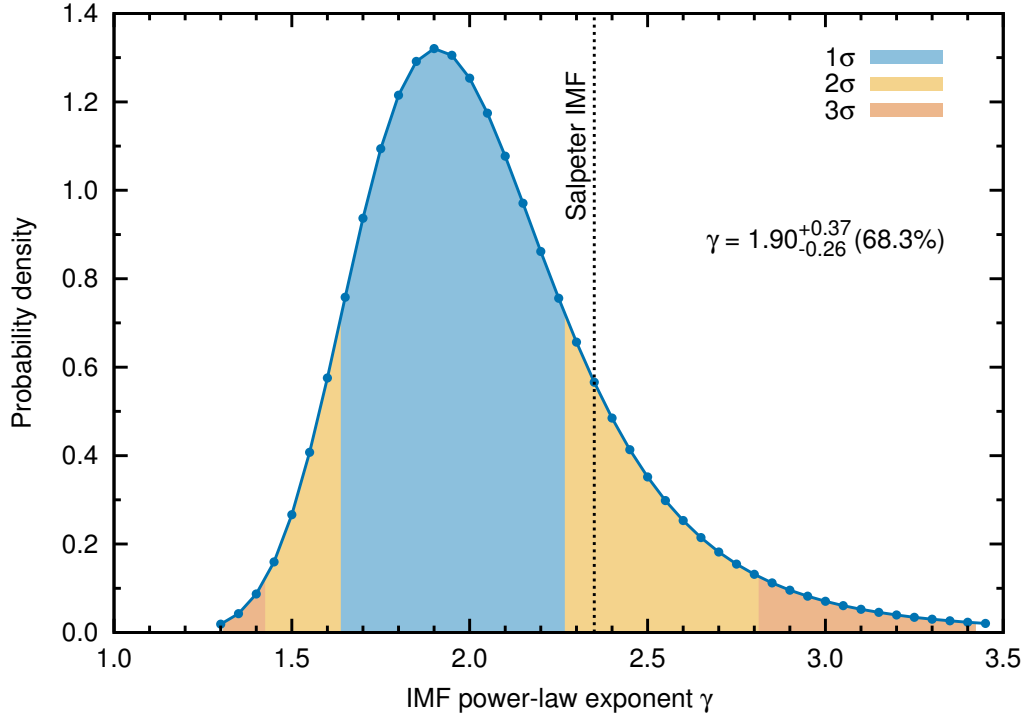


Figure 6. Probability density distribution of the slope of the IMF (Schneider et al. 2017).

trosopic binaries (Ramírez-Agudelo et al. 2015). This suggests that binary interactions need to be accounted for to understand the underlying rotational distribution.

The VFTS results also indicate that the main-sequence needs widening. This hints at a larger value for the core overshooting parameter than usually adopted. Finally, VMS up to at least $200M_{\odot}$ are common in 30 Dor, but VMS mass-loss rates have been *underestimated*.

References

- Bestenlehner, J. M., Gräfener, G., Vink, J. S., et al. 2014, *A&A*, 570, A38
 Brott, I., de Mink, S. E., Cantiello, M., et al. 2011, *A&A*, 530, A115
 Crowther, P. A., Schnurr, O., Hirschi, R., et al. 2010, *MNRAS*, 408, 731
 Doran, E. I., Crowther, P. A., de Koter, A., et al. 2013, *A&A*, 558, A134
 Evans, C. J., Taylor, W. D., Hénault-Brunet, V., et al. 2011, *A&A*, 530, A108
 Gies, D. R., & Bolton, C. T. 1986, *ApJS*, 61, 419
 Grin, N. J., Ramírez-Agudelo, O. H., de Koter, A., et al. 2016, arXiv:1609.00197
 Hillier, D. J., & Miller, D. L. 1998, *ApJ*, 496, 407
 Hunter, I., Lennon, D. J., Dufton, P. L., et al. 2008, *A&A*, 479, 541
 Keszthelyi, Z., Puls, J., & Wade, G. A. 2017, *A&A*, 598, A4
 Köhler, K., Langer, N., de Koter, A., et al. 2015, *A&A*, 573, A71
 Kudritzki, R.-P., & Puls, J. 2000, *ARA&A*, 38, 613
 Langer, N. 2012, *ARA&A*, 50, 107
 Martins, F. 2015, *Very Massive Stars in the Local Universe*, 412, 9
 McEvoy, C. M., Dufton, P. L., Evans, C. J., et al. 2015, *A&A*, 575, A70
 Mokiem, M. R., de Koter, A., Evans, C. J., et al. 2007, *A&A*, 465, 1003
 Muijres, L. E., de Koter, A., Vink, J. S., et al. 2011, *A&A*, 526, A32

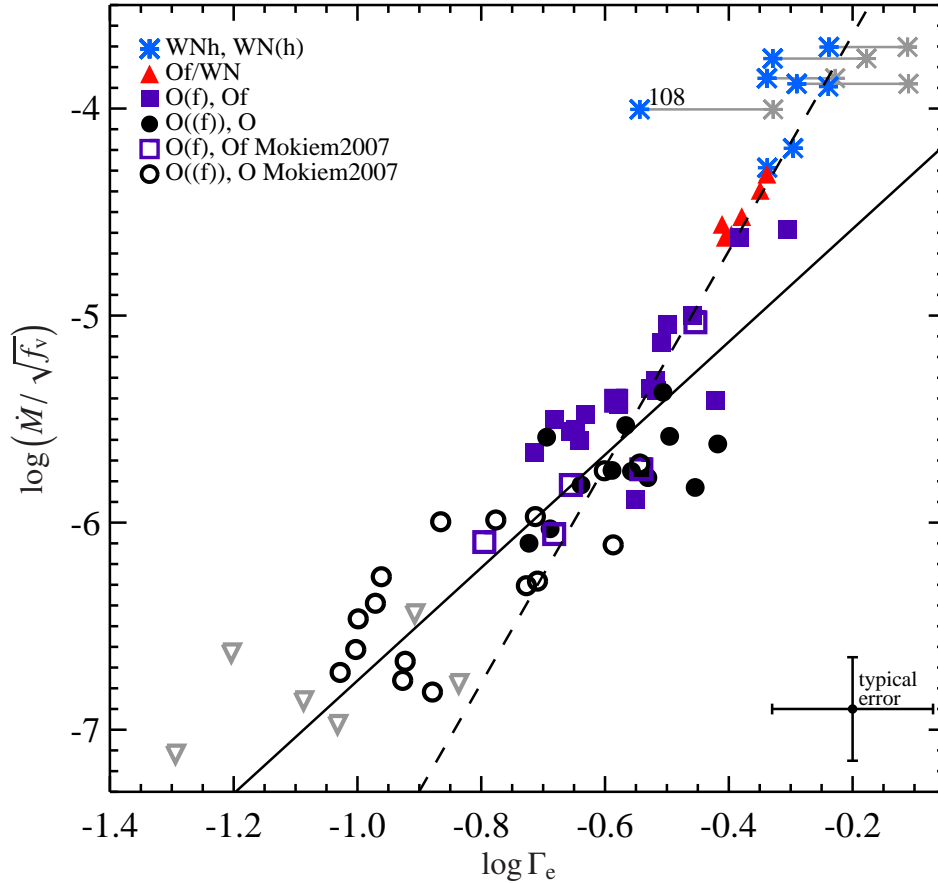


Figure 7. Unclumped $\log \dot{M}$ vs. $\log \Gamma_e$. Solid line: $\dot{M} - \Gamma$ relation for O stars. The different symbols indicate stellar sub-classes from Bestenlehner et al. (2014). Dashed line: the steeper slope of the Of/WN and WNh stars. The *kink* occurs at $\log \Gamma_e = -0.58$. The grey asterisks indicate the position of the stars with $Y > 0.75$ under the assumption of core He-burning. The grey upside down triangles are stars from Mokiem et al. (2007) which only have upper limits and are excluded from the fit. Note the presence of a *kink*, as predicted by Vink et al. (2011).

- Petrov, B., Vink, J. S., & Gräfener, G. 2016, MNRAS, 458, 1999
Puls, J., Urbaneja, M. A., Venero, R., et al. 2005, A&A, 435, 669
Puls, J., Vink, J. S., & Najarro, F. 2008, A&Ar, 16, 209
Ramírez-Agudelo, O. H., Simón-Díaz, S., Sana, H., et al. 2013, A&A, 560, A29
Ramírez-Agudelo, O. H., Sana, H., de Mink, S. E., et al. 2015, A&A, 580, A92
Ramírez-Agudelo, O. H., Sana, H., de Koter, A., et al. 2017, arXiv:1701.04758
Rivero González, J. G., Puls, J., Najarro, F., & Brott, I. 2012, A&A, 537, A79
Sabín-Sanjulián, C., Simón-Díaz, S., Herrero, A., et al. 2014, A&A, 564, A39
Sana, H., de Koter, A., de Mink, S. E., et al. 2013, A&A, 550, A107
Stone, R. C. 1991, AJ, 102, 333
Sundqvist, J. O., Puls, J., & Owocki, S. P. 2014, A&A, 568, A59
Šurlan, B., Hamann, W.-R., Aret, A., et al. 2013, A&A, 559, A130
Vink, J. S., & Gräfener, G. 2012, ApJL, 751, L34
Vink, J. S., de Koter, A., & Lamers, H. J. G. L. M. 2001, A&A, 369, 574
Vink, J. S., Brott, I., Gräfener, G., et al. 2010, A&A, 512, L7
Vink, J. S., Heger, A., Krumholz, M. R., et al. 2015, Highlights of Astronomy, 16, 51